THE JOURNAL OF PHYSICAL CHEMISTRY B

Article

pubs.acs.org/JPCB

Liquid–Liquid Interface Motion of a Capsule Motor Powered by the Interlayer Marangoni Effect

Guanjia Zhao and Martin Pumera*

Division of Chemistry & Biological Chemistry, School of Physical and Mathematical Sciences, Nanyang Technological University, 21 Nanyang Link, 637371 Singapore

Supporting Information

ABSTRACT: A novel thin capsule motor has been described in this report. It utilizes the Marangoni effect for the solid capsule to run at a water–oil interlayer, which has not been reported previously. Intrinsic and environment factors influencing the motion were investigated. It is also possible for the velocity, direction, and start/stop of the motion of the capsule to be manipulated.

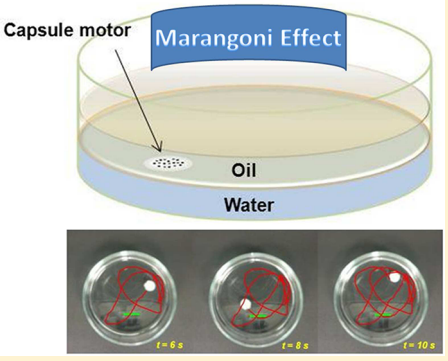

INTRODUCTION

There is a strong interest in autonomous, self-propelled, and self-powered nano-, milli-, and micromachines which can mimic and outperform biological systems.[1−3] The energy sources for such machines can be from an external energy field,[4−6] through consumption of fuels,[3] or via physicochemical processes,[7] which is the so-called Marangoni effect. The Marangoni effect describes the movement of the object based on surface tension gradient. This surface tension gradient can be generated by asymmetric release of the chemical from the object[8,9] or by modification of the surface the object moves on.[10,11] Considerable promises for such autonomous devices are given in the areas of biomedical applications,[2,12] environmental remediation,[7,13] as well as discovery of natural resources.[14] Artificial nano-, micro-, and millimeter self-powered systems are able to autonomously translate on the inside of the liquid,[15,16] liquid/air,[17−19] liquid/solid,[20,21] or solid/air[22,23] interfaces. However, up until now, there has not been any demonstration of an autonomous system which is able to translate at the liquid/liquid interface and only the spreading of liquid at such interface was reported.[24] Here we wish to show for the first time that a millimeter-sized capsule motor can identify the liquid/liquid interface and autonomously move at this interface. We hereby report the intrinsic and environmental factors which influence the movement of the capsule motor.

RESULTS AND DISCUSSION

We prepared the liquid/liquid interface based on an oil/water system in a Petri dish as depicted in Scheme 1. Oil has a lower density than water and thus it interfaced with air as well. A solution of polysulfone polymer (PSf) in *N*,*N*′-dimethylformamide (DMF) was prepared, and a volume of 5 μL of PSf/DMF solution was dropped on the oil surface of the oil/water system. The PSf/DMF droplet penetrated the oil layer because it was immiscible with oil and has a density higher than that of oil. Upon contact with the underlying aqueous phase at the oil/water interface, PSf solidified immediately via a phase inversion

Scheme 1. Illustration of the Capsule Motor at the Oil–Water Interface[a]

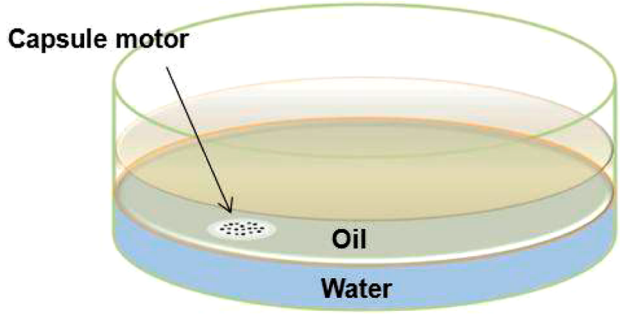

[a]When the polysulfone-DMF solution penetrated through the oil layer, polysulfone solidified immediately upon interaction with water. The capsule motor was thus formed. The top surface of the capsule motor appeared to be quite porous, and DMF molecules were released out through the pores. Motion was initiated consequently within 0.15–0.2 s as the asymmetrical releasing of DMF created an imbalanced surface concentration and surface energy around the capsule motor.

Received: June 13, 2012
Revised: August 10, 2012
Published: August 15, 2012

mechanism,[25] creating a thin capsule motor. This process is illustrated in Figure 1A.

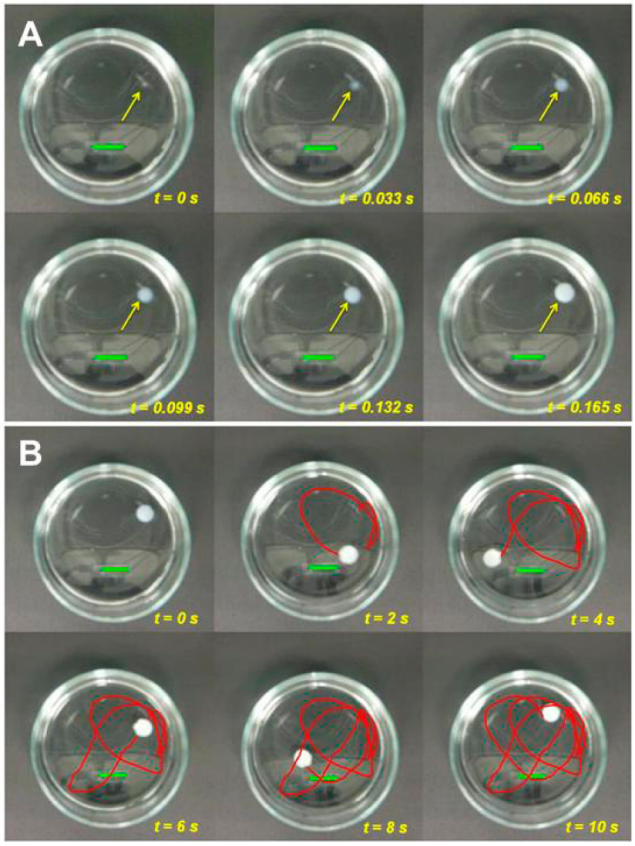

Figure 1. (A) Formation process of the capsule motor. Snapshots were taken with a time interval of 0.033 s. (B) Tracking images of the motion of a capsule motor with a time interval of 2 s. The scale bar indicates 1 cm. The film underwent only translational motion, and spinning or circularization of the film were not observed.

It took approximately 0.165 s for the PSf molecules to completely interact with water and form the solid-state framework of the capsule motor. The increment of size indicated the growth and formation process of the structure. The autonomous movement of the capsule began immediately after the capsule was formed at the oil/water interface. The movement of the capsule motor was driven by the asymmetric release of DMF from the capsule via an interlayer Marangoni effect. The capsule releases DMF, which is miscible with water. Since DMF exhibits a much lower surface tension (γ = 35.2 mN m^{-1}) than water (γ = 72.0 mN m^{-1}), the capsule is pulled toward the direction of solution with higher surface tension.[7] It should be noted that the capsule movement is influence by the friction originating from the aqueous phase and, in addition, also from the oil layer. Tracking of motion is illustrated in Figure 1B. As the capsule motor released DMF asymmetrically to the aqueous phase, the difference in surface tension at the opposite side of the capsule resulted in the motion of the motor.

The capsule motor had a typical diameter of 6 mm with a thickness of 830 μm and exhibited a maximum velocity of 7.5 cm/s, which was equivalent to a speed of 12.5 bodylengths/s (bd/s). The duration of translational movement of the capsule motor at the oil/water interface was 0.5−1.5 min, reaching a maximum traveled distance of 57 cm. Upon analyzing the morphology of the capsule motor by scanning electron microscopy (SEM), we found that the side exposed to the oil layer exhibited large pores of ∼35 μm while the side exposed to water, in contrary, did not have any large porous features but has a compact solid appearance instead, even at a high magnification (Figure S1 in the Supporting Information). This is due to the fact that when PSf/DMF solidified at the oil/water interface, it underwent a fast phase inversion with contact with water, and when PSf solidified while at the oil interface, the phase inversion did not take place. This is similar to the morphology of the capsules we previously observed at the air/water system interface.[7] The motion of the capsule motor was facilitated by an asymmetric release of the encapsulated DMF in the PSf capsule which released slowly into the water at the interface and thus created a difference in the surface tension surrounding the capsule motor.

We have studied several factors that influence the motion of the capsule motor at the oil/water interface. Two important factors have to be considered, mainly (i) the driving force and (ii) the friction force. From the driving force point of view, the motion is caused by the mixing of DMF molecules with water, which is affected by the releasing speed of DMF from the capsule. We varied the PSf concentration in DMF for a constant volume of the precursor, that is, the PSf/DMF solution (5 μL). The measured velocity decreased with a higher amount of PSf in DMF. This is due to a slower release of DMF and thus smaller difference in surface tension in the vicinity of the capsule motor (Figure 2A). Simultaneously during the motion, the capsule motor experienced a friction force from both the water and oil media. We varied the size of the capsule by varying the volume of the precursor solution of PSf/DMF. As the diameter of the capsule motor increased, the speed decreased since the capsule experienced a larger friction force from the liquid media (Figure 2B). As such, through variation of the concentration of PSf in DMF or the volume of the precursor, we can engineer the capsule motor for the designing of its velocity. We also investigated the influence of the surface tension of aqueous media on the movement of the capsule motor. As the movement is driven by the surface tension difference between the released DMF (γ = 35.2 mN/m) and that of the aqueous media, the velocity of the capsule motor should decrease when the surface tension of the aqueous solution decreases. When the surface tension of the aqueous solution is equal to the surface tension of DMF, the velocity of the capsule motor should be zero as the Marangoni effect provides the driving force for the movement. We varied the surface tension of the aqueous phase by the introduction of acetic acid; the surface tension of water (γ = 72.0 mN/m) decreases with an increasing amount of acetic acid in the solution, i.e., to 36.1 mN/m at 60% and 33.5 mN/m at 70% (v/v). In concordance with our prediction, we observed that the average velocity of the capsule motors decreased with a higher concentration of acetic acid in the aqueous phase, since the surface tension difference between the DMF and aqueous phase decreased. The movement of the capsule motor stopped at the 60% acetic acid/oil system, demonstrating that the force originating from the surface tension difference is not capable of overcoming the drag force of the system (Figure 2C).

Along with autonomous movement, it is also of high importance for any motor to exhibit a start/stop behavior. In Figure 3A,B, we demonstrated that we were able to dock and release the capsule motor loaded with nickel nanoparticles

dx.doi.org/10.1021/jp3057702 | J. Phys. Chem. B 2012, 116, 10960−10963

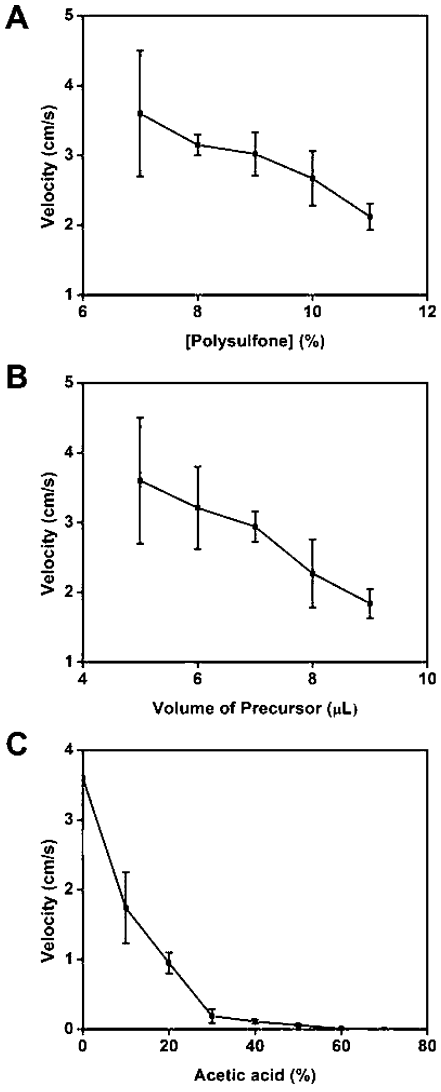

Figure 2. Velocity of the capsule motor varies with (A) loading of polysulfone in the precursor solution, (B) volume of the PSf/DMF precursor solution, and (C) concentration of acetic acid in the aqueous phase.

using an external magnetic field. From t = 0 s to t = 1 s, no magnet was present and motion of the capsule was tracked and measured. From t = 1 s to t = 2 s, a magnet bar was placed underneath the Petri dish, and the movement of the capsule motor was paused with the capsule motor and appeared to be docked at the desired location. From t = 2 s to t = 3 s, the magnet bar was removed and the movement could be resumed. We also demonstrated the directionality of the movement of the capsule motor by placing the magnet at the side of the Petri dish. The capsule motor exhibited preferential movement toward the source of the magnetic field. As shown in Figure 3C, with the magnet bar placed at one side (top of the image), the overall direction of the motor was toward the magnet bar, instead of being random.

CONCLUSIONS

In conclusion, we have demonstrated for the first time a self-propelled motor on a liquid/liquid interface. The precursor of the capsule motor penetrates the oil layer, and the capsule motor is formed upon contact with an aqueous phase. The

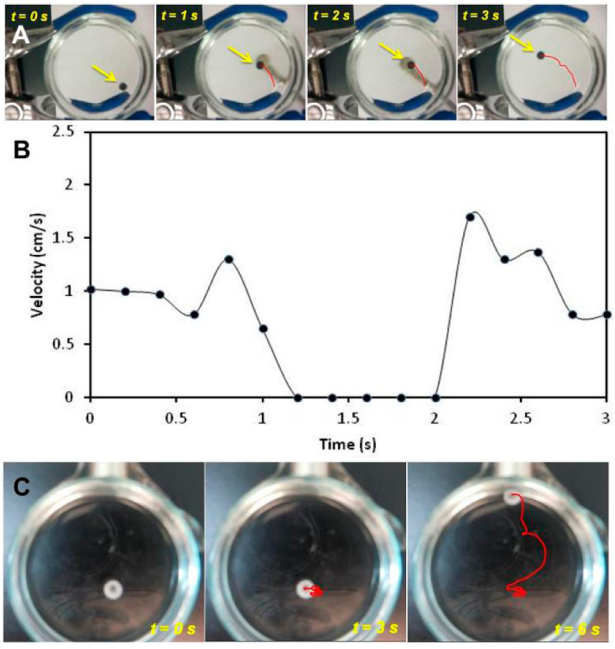

Figure 3. Manipulation of the motion of the capsule motor with the magnetic field: (A) tracking images of the motion of a nickel NP incorporated capsule motor with a time interval of 1 s, (B) instant velocity to show the start and stop control of the motion, and (C) directional control of the velocity with a magnetic bar.

motor movement originates from an interphase Marangoni effect. We have shown that the movement of the capsule motor can be controlled by applying a magnetic field. We believe that our findings open the door for a new research field of movement of milli-, micro-, and nanomotors at the liquid/liquid interface.

EXPERIMENTAL SECTION

The experiments were carried out in 50 mm diameter Petri dishes of a height of 14 mm. A volume of 10 mL of mineral oil (Singer) was placed on top of 10 mL of aqueous phase liquid. A Casio HD videorecorder was placed over the dish. Precursor solution of the capsule was prepared by mixing polysulfone (CAS 25135-51-7; $C_{27}H_{22}O_4S$; M_r = 22 000; Sigma-Aldrich, catalog no. 182443) with *N*,*N*′-dimethylformamide (Merck) and was dissolved into a clear solution using an ultrasonic bath for 30 min. A droplet of PSf/DMF solution was applied on the surface of oil with a pipet, and it slowly penetrated through the oil layer and solidified at the oil−water interface. The motion of the capsule started immediately when the capsule was formed. For the Ni-containing capsules, 5 wt % of nickel nanoparticles (50 nm diameter; Sigma-Aldrich) was incorporated into the PSf/DMF solution by mixing of PSf/DMF solution with Ni NPs. A droplet of Ni/PSf/DMF suspension was dropped on the surface of the oil. After penetrating through the oil layer and solidifed, the capsule was formed with Ni nanoparticles trapped inside. Motion of the capsule starts at the same time. A permanent magnet was placed near the Petri dish to manipulate the motion of Ni-incorporated capsules. The capsule was immediately attracted toward the magnet due to the presence of Ni nanoparticles. The video sequences of the videos were analyzed using Nikon NIS-Elements software, and the average velocities over the first 10 s were calculated. For each set of data, the standard deviation and average value of the recorded

dx.doi.org/10.1021/jp3057702 | J. Phys. Chem. B 2012, 116, 10960−10963

velocities (n = 5) were calculated with the standard deviations shown as error bars.

■ ASSOCIATED CONTENT

Supporting Information

Scanning electron microscopy (SEM) images for the surface morphology characterization of capsules. This material is available free of charge via the Internet at http://pubs.acs.org.

■ AUTHOR INFORMATION

Corresponding Author

*Fax: (65) 6791-1961. E-mail: pumera@ntu.edu.sg.

Notes

The authors declare no competing financial interest.

■ REFERENCES

(1) Balasubramanian, S.; Kagan, D.; Hu, C.-M. J.; Campuzano, S.; Lobo-Castañon, M. J.; Lim, N.; Kang, D. Y.; Zimmerman, M.; Zhang, L.; Wang, J. *Angew. Chem., Int.Ed.* **2011**, *50*, 4161−4164.
(2) Paxton, W. F.; Sundararajan, S.; Mallouk, T. E.; Sen, A. *Angew. Chem., Int. Ed.* **2006**, *45*, 5420−5429.
(3) Sanchez, S.; Ananth, A. N.; Fomin, V. M.; Viehrig, M.; Schmidt, O. G. *J. Am. Chem. Soc.* **2011**, *133*, 14860−14863.
(4) Loget, G.; Kuhn, A. *J. Am. Chem. Soc.* **2010**, *132*, 15918−15919.
(5) Loget, G.; Kuhn, A. *Nat. Commun* **2011**, *2*, 535.
(6) Loget, G.; Kuhn, A. *Lab Chip* **2012**, *12*, 1967−1971.
(7) Zhao, G.; Seah, T. H.; Pumera, M. *Chem.—Eur. J.* **2011**, *17*, 12020−12026.
(8) Jin, H.; Marmur, A.; Ikkala, O.; Ras, R. H. A. *Chem. Sci.* **2012**, *3*, 2526−2529.
(9) Sharma, R.; Chang, S. T.; Velev, O. D. *Langmuir* **2012**, *28*, 10128−10135.
(10) Chaudhury, M. K.; Whitesides, G. M. *Science* **1992**, *256*, 1539−1541.
(11) Zhao, G.; Pumera, M. *Chem. Asian J.* **2012**, *7*, 1994.
(12) Sanchez, S.; Solovev, A. A.; Schulze, S.; Schmidt, O. G. *Chem. Commun.* **2011**, *47*, 698−700.
(13) Zhao, G.; Stuart, E. J. E.; Pumera, M. *Phys. Chem. Chem. Phys.* **2011**, *13*, 12755−12757.
(14) Hong, Y.; Velegol, D.; Chaturvedi, N.; Sen, A. *Phys. Chem. Chem. Phys.* **2010**, *12*, 1423−1435.
(15) Sanchez, S.; Solovev, A. A.; Mei, Y.; Schmidt, O. G. *J. Am. Chem. Soc.* **2010**, *132*, 13144−13145.
(16) Sanchez, S.; Solovev, A. A.; Harazim, S. M.; Schmidt, O. G. *J. Am. Chem. Soc.* **2010**, *133*, 701−703.
(17) Diguet, A.; Guillermic, R.-M.; Magome, N.; Saint-Jalmes, A.; Chen, Y.; Yoshikawa, K.; Baigl, D. *Angew. Chem., Int. Ed.* **2009**, *48*, 9281−9284.
(18) Okawa, D.; Pastine, S. J.; Zettl, A.; Fréchet, J. M. J. *J. Am. Chem. Soc.* **2009**, *131*, 5396−5398.
(19) Luo, C.; Li, H.; Liu, X. *J. Micromech. Microeng.* **2008**, *18*, 067002.
(20) Paxton, W. F.; Baker, P. T.; Kline, T. R.; Wang, Y.; Mallouk, T. E.; Sen, A. *J. Am. Chem. Soc.* **2006**, *128*, 14881−14888.
(21) Valadares, L. F.; Tao, Y.-G.; Zacharia, N. S.; Kitaev, V.; Galembeck, F.; Kapral, R.; Ozin, G. A. *Small* **2010**, *6*, 565−572.
(22) Sumino, Y.; Magome, N.; Hamada, T.; Yoshikawa, K. *Phys. Rev. Lett.* **2005**, *94*, 068301.
(23) Schmid, A. K.; Bartelt, N. C.; Hwang, R. Q. *Science* **2000**, *290*, 1561−1564.
(24) Berg, S. *Phys. Fluids* **2009**, *21*, 032105.
(25) Sanchez, S.; Roldan, M.; Perez, S.; Fabregas, E. *Anal. Chem.* **2008**, *80*, 6508−6514.